Climate Dynamics
https://doi.org/10.1007/s00382-020-05133-5

The MJO's impact on rainfall trends over the Congo rainforest

Ajay Raghavendra[1] · Liming Zhou[1] · Paul E. Roundy[1] · Yan Jiang[1] · Shawn M. Milrad[2] · Wenjian Hua[3] · Geng Xia[4]

Received: 13 August 2019 / Accepted: 13 January 2020

Abstract
A significant declining trend in rainfall over the Congo basin has been observed over the past three decades. Since the Madden–Julian oscillation (MJO) is a major forcing mechanism for tropical convection and rainfall, the interannual variability and trend in rainfall over the Congo may be partly attributable to variability or changes in the MJO. This study explores the long-term (1979–2018) relationship between the active MJO diagnosed by the real-time multivariate (RMM) MJO phase index data and observed rainfall and cloud data over the Congo during October–March. Since the MJO may significantly enhance rainfall during the wet phases or suppress rainfall during the dry phases, the crux of this paper includes how trends in MJO activity may impact the overall observed precipitation trend over the Congo. The relationship between MJO activity and rainfall over the Congo was documented using statistical techniques and composite analysis. A new, yet simple approach was developed to partition seasonal rainfall depending on the MJO phase (i.e., wet, dry, inactive, and other). Results show a significant correlation between the number of wet and dry MJO days, and rainfall enhancement and suppression over the Congo. While there exists considerable interannual variability in MJO activity and rainfall over the Congo, there is a significant increase in the number of dry MJO days (3.47 days decade^{-1}) which tends to intensify the large-scale drying trend over the Congo during October–March. The increasing trend in the number of dry MJO days is likely enhancing the net drying trend by 13.6% over the Congo.

Keywords Congo rainforest · Madden–Julian oscillation (MJO) · Rainfall trend · Tropical rainbelt

1 Introduction

Tropical rainforests play an important role in regulating the Earth's climate system. For example, rainforests help mitigate human caused global warming by acting as a global carbon sink (e.g., Lewis 2006; Lewis et al. 2009). While there has been considerable recent works to understand climate change and variability over the Congo rainforests, the physical mechanisms involved are only partially understood (e.g., Hua et al. 2018; Jiang et al. 2019). This knowledge gap is further aggravated over Africa (especially the Congo) due to the relative lack of fundamental research and absence of field measurements (e.g., Washington et al. 2013; Lee and Biasutti 2014; Alsdorf et al. 2016) when compared to other parts of the world including the Congo's counterpart the Amazon rainforest (Alsdorf et al. 2016).

Recent studies have documented a large-scale and long-term drying trend during the past three decades over the Congo rainforest located in Equatorial Africa (e.g., Zhou et al. 2014; Hua et al. 2016, 2018; Jiang et al. 2019). This long-term drought is principally responsible for the significant loss of vegetation greenness and canopy water content during the rainfall transition season of April–June (Zhou et al. 2014) and a widespread increase of boreal summer dry season (June–August) length (Jiang et al. 2019) over the Congo. Naturally, these changes have raised important questions pertaining to the physical mechanisms responsible for the drought, and concerns about the future of the Congo

✉ Ajay Raghavendra
araghavendra@albany.edu

[1] Department of Atmospheric and Environmental Sciences, University at Albany, Albany, NY, USA

[2] Meteorology Program, Applied Aviation Sciences Department, Embry-Riddle Aeronautical University, Daytona Beach, FL, USA

[3] Key Laboratory of Meteorological Disaster, Ministry of Education, Nanjing University of Information Science and Technology, Nanjing 210044, China

[4] National Renewable Energy Laboratory, National Wind Technology Center, Golden, CO, USA

Published online: 28 January 2020

forest, agricultural activity, and socio-economic implications for Central-Equatorial Africa (CEA).

Possible mechanisms responsible for the drought over the Congo have been explored in the past several years. Hua et al. (2016) studied trends and patterns in tropical sea surface temperatures (SSTs) and reported the enhancement and westward shift of the descending branch of the tropical Walker circulation has increased subsidence over the Congo and subsequently resulted in a decline in rainfall. This finding was further substantiated in a follow-up study using climate models (Hua et al. 2018). A strong link was also found between the Indian Ocean Dipole (IOD), Walker circulation and convection over the maritime continents, and rainfall over the Congo using Coupled Model Intercomparison Project (CMIP5; Taylor et al. 2012) models (Creese et al. 2019). Interestingly, satellite observations show an increase in thunderstorm activity and intensity (Raghavendra et al. 2018). This unintuitive relationship between intensifying thunderstorm activity and decrease in rainfall over the Congo may be reconciled by applying the conclusions of other studies (e.g., Hamada et al. 2015) who found that the tallest and most intense thunderstorms do not produce the most rainfall in the tropical latitudes (especially over land). Needless to say, thunderstorms are essential for rainfall over the Congo (e.g., Jackson et al. 2009; Hamada et al. 2015; Taylor et al. 2017, 2018).

There exists agreement on some dynamic and thermodynamic responses to global warming in climate models (Held and Soden 2006). However, important sources of seasonal/sub-seasonal variability (e.g., the Madden–Julian Oscillation or MJO), tropical convection, rainfall characteristics, and associated large scale dynamics are poorly resolved by climate models (e.g., Dai 2006; Hung et al. 2013; Chen and Dai 2019). Therefore, climate models cannot explain the entirety of the rainfall trend over the Congo and thus resulting in uncertainties for future climate projections over the Congo. Even climate models forced with observed SSTs struggle to replicate the strong drying trend over the Congo (e.g., Hua et al. 2018). Therefore, changes and variability in seasonal to sub-seasonal processes such as the MJO, Kelvin waves (Sinclaire et al. 2015), and other tropical waves (Raghavendra et al. 2019) which are important mechanisms that influence tropical convection and precipitation are poorly simulated by climate models, and an important source of uncertainty in climate models and future climate projections.

While climate models perform modestly in simulating tropical waves (Hung et al. 2013), long-term satellite observations have suggested an increase in high-frequency variability and a decrease in low-frequency variability in Convectively Coupled Atmospheric Equatorial Waves (CCAEWs; Raghavendra et al. 2019). While the variability between CCAEWs and precipitation has been previously studied (e.g., Sinclaire et al. 2015), trends in the relationship between CCAEWs and precipitation has received little attention. Furthermore, while the role of the MJO and other tropical waves on rainfall over Africa has been previously investigated, these studies have usually limited their domain of interest to Southern Africa (e.g., Pohl et al. 2018), Western Africa/Sahel (Schlueter et al. 2019a, b), or Eastern Africa (e.g., Pohl and Camberlin 2006a, b; Berhane and Zaitchik 2014). This has resulted in a lack of understanding of the MJO's impact over CEA (especially the Congo rainforest).

Since the MJO (Madden and Julian 1971, 1972) is an important dynamic–thermodynamic mechanism connected to the variability in the large-scale circulation of the tropics and extra-tropics, and modulates rainfall, we need to study changes in MJO activity and associated rainfall impacts as a possible contributor to the overall rainfall drying trend over the Congo rainforest. Understanding the mechanisms for the phasing between the MJO and the tropical rainbelt over Africa is also motivated by a declining trend in spectral power (variance) corresponding to the MJO frequency–wavenumber band (Raghavendra et al. 2019). Given the importance of the Congo rainforest and the potential impact MJOs have in modulating tropical rainfall, this paper studies the long-term (1979–2018) relationship between the MJO and precipitation over the Congo rainforest using observations and reanalysis data. The impact of trends in MJO activity on rainfall over the Congo are also investigated in this study.

2 Data

In this study, four datasets detailed below which are available at daily or higher temporal resolution from 1979–2018 (40-year period) and 1983–2018 (36 years) were used:

1. The daily MJO RMM phase index data (Wheeler and Hendon 2004) were obtained from the Bureau of Meteorology (Australia) website (http://www.bom.gov.au/climate/mjo/). The RMM index is better suited to evaluate rainfall over the Congo when compared to other MJO indices (e.g., outgoing longwave radiation-based MJO Index–OMI) because it incorporates the lower- and upper-tropospheric zonal wind, which influence vertical motion over Africa through interaction with topography or through confluence of flow. Also, outgoing longwave radiation (OLR) has a smaller impact compared to the upper and lower tropospheric zonal windfield on the MJO RMM index (Wheeler and Hendon 2004), and OLR is poorly correlated with rainfall over the Congo and other parts of Africa (e.g., Schlueter et al. 2019a). Furthermore, the RMM index is widely used and hence makes it easier to relate the research presented in this paper with previous works. As suggested by previous

studies (e.g., LaFleur et al. 2015), days with an MJO amplitude ≥ 1 were regarded as active MJO days, and days with an MJO amplitude < 1 were regarded as inactive MJO days. RMM phase 2 was regarded as the wet phase (enhanced rainfall), and phases 5 and 6 were regarded as the dry phases (suppressed rainfall) for Equatorial Africa (Gottschalck et al. 2010; Raghavendra et al. 2017; Zaitchik 2016). These RMM phase combinations to define the wet and dry MJO regimes yielded the most significant distinction between wet and dry conditions (Fig. 1). Furthermore, sensitivity tests for other practical choices and combinations for wet or dry RMM phases (e.g., phases 1 and 2 for wet MJO days, or phases 4 and 5 for dry MJO days) did not qualitatively impact the arguments and conclusions presented in this paper.

2. The NOAA Climate Prediction Center (CPC) global unified gauge-based daily precipitation data (in mm day^{-1}) was obtained from NOAA/OAR/ESRL/PSD website (https://www.esrl.noaa.gov/psd/) at 0.5° horizontal resolution. The daily mean precipitation over the Congo was calculated by spatially averaging the precipitation between 7.75° N–7.75° S and 12.25° E–32.75° E (study region depicted by a dashed green line in Fig. 2b). The rainfall estimates from this dataset compared well to other datasets such as the Global Precipitation Climatology Centre (GPCC) and a new observational precipitation dataset (NIC131) developed by Nicholson et al. (2018) over the Congo region. However, unlike GPCC and NIC131 where the long-term record is only available at monthly resolution, the CPC global unified gauge-based analysis is available at a daily temporal and relatively higher spatial resolution.
3. Rainfall variability over the Congo Basin is closely linked to the large-scale atmospheric circulation in the lower- and middle-troposphere (Hua et al., 2019). The 850 hPa zonal (u) and meridional (v) wind data every 6-h at 0.7° horizontal grid resolution were obtained from the European Centre for Medium-Range Weather Forecast (ECMWF) interim reanalysis (ERA-I; Dee et al. 2011). This 6-h data was converted to daily (24-h) temporal resolution since the RMM phase and precipitation datasets are only available at daily resolution. The hori-

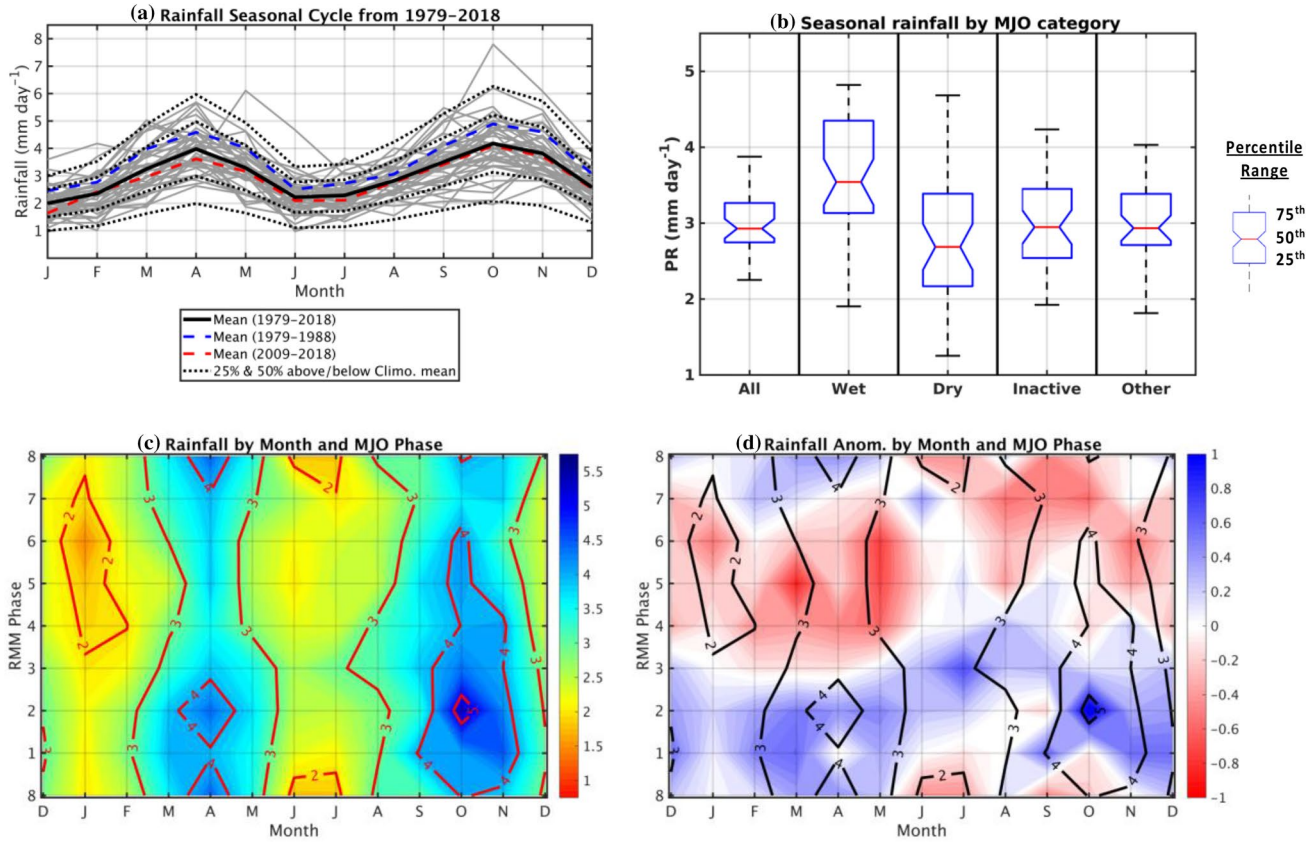

Fig. 1 **a** Seasonal cycle of rainfall over the Congo using daily CPC rainfall data (see plot legend for details). **b** Boxplot showing the average seasonal rainfall by MJO category. **c** Mean and **d** anomalous rainfall (shaded in mm day^{-1}) for each month and RMM phase. In **b**, non-overlapping notches indicate that the true medians differ at the 95% confidence level, and the top and bottom whiskers indicate the maximum and minimum values. Days with an RMM amplitude < 1 are omitted in **b–d**

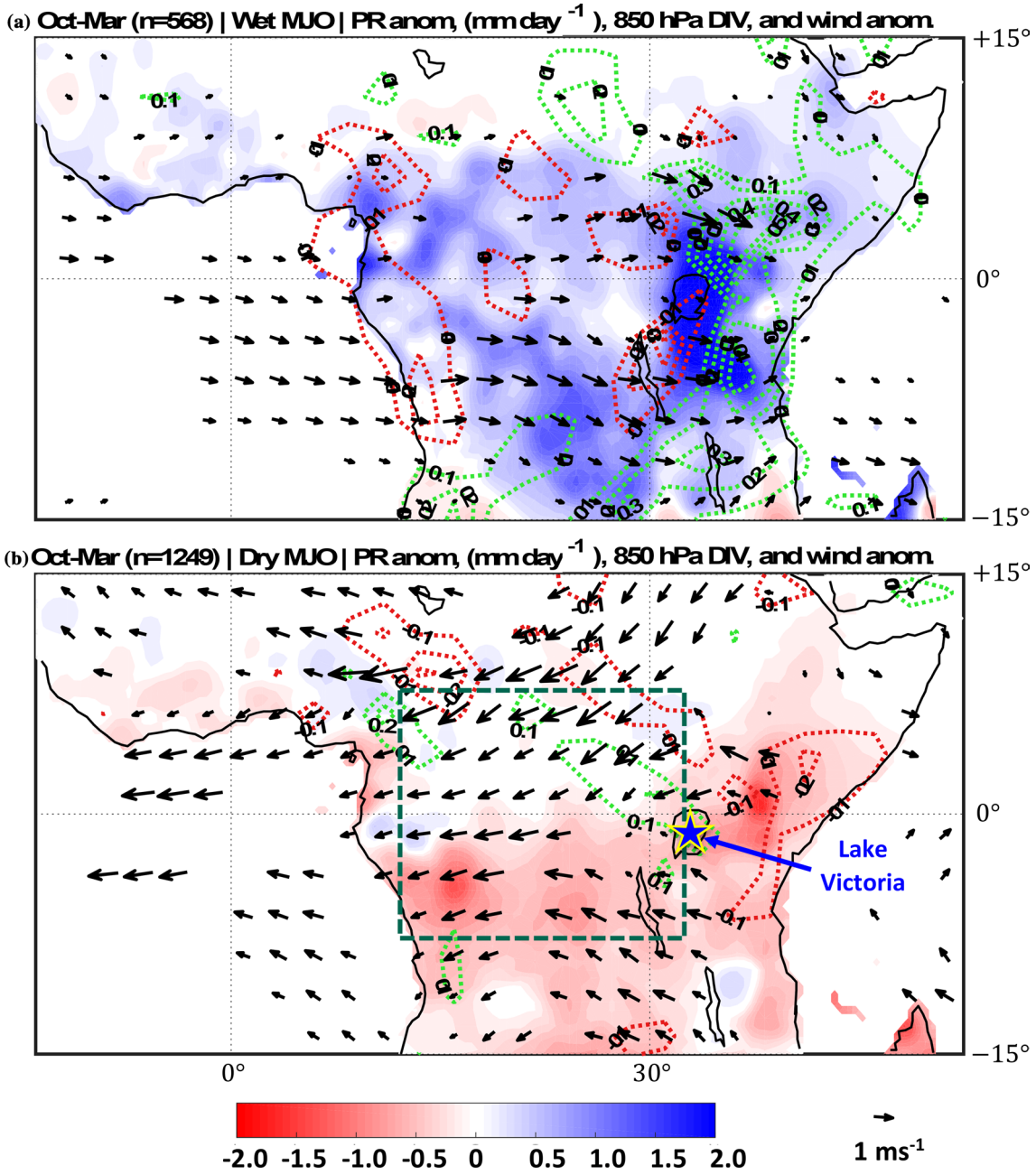

Fig. 2 CPC daily rainfall anomaly, ERA-I 850 hPa divergence (dotted red), convergence (dotted green) and vector wind anomalies for **a** wet MJO days, and **b** dry MJO days during Oct–Mar from 1979–2018. Wind vectors are shown only when significantly different from the Oct–Mar climatology at the 10% level using bootstrapping. The domain representative of the Congo rainforest in shown in dashed green in panel **b**

zontal resolution was reduced by interpolating the data onto a 2.5° grid to focus on large-scale circulation. The wind divergence anomaly field i.e., $-(\partial u'/\partial x + \partial v'/\partial y)$ (where x and y are the latitudinal and longitudinal directions, and $'$ indicates anomaly from the seasonal mean) was calculated to assess different circulation patterns associated with RMM phases using composite analysis. Since the composite analysis is centered around the RMM phases from different MJO events with large variability in the background meteorological conditions, statistical significance testing for the seasonal composites was performed by using a bootstrap random re-sampling tests with 1000 iterations (e.g., Ventrice et al. 2012; Sinclaire et al. 2015). Other reanalysis products could be used in this study but it is difficult to identify the "best" reanalysis dataset over the Congo Basin given the lack of

surface observations and radiosonde network (Washington et al. 2013; Hua et al. 2019). Nevertheless, the bias and root-mean-square error associated with the ERA-I windfield is comparable with other datasets (Hua et al. 2019) and hence the ERA-I is suitable for this study.

4. Rainfall over the Congo relies on thunderstorm activity (e.g., Jackson et al. 2009; Hamada et al. 2015; Taylor et al. 2017, 2018). Given limited rainfall observations available over the Congo (e.g., Alsdorf et al. 2016; Nicholson et al. 2018), here we use the areal extent of satellite measured cloudiness as an independent proxy for rainfall activity to confirm our results from the CPC dataset. Cold cloud top cover indicative of thunderstorm activity was evaluated using infrared (IR) brightness temperature (T_b) < −40 °C from the gridded satellite (GridSat-B1) dataset (Knapp 2008; Knapp et al. 2011) from 1986–2018. Daily mean cloud cover was obtained by calculating the number of pixels with T_b < −40 °C between 5° N–5° S and 12° E–30° E during 18:00 and 21:00 UTC. A slightly smaller domain was chosen for the cloud analysis since heatmaps for thunderstorms and lightning activity show significantly higher activity over the Congo basin (e.g., Zipser et al. 2006). Rainfall on the other hand was evaluated over a larger domain since precipitation occurring near the edges of the Congo basin at higher elevations are orographically forced into the Congo basin. We choose the GridSat-B1 IR channel T_b as it satisfies Climate Data Record (CDR) program quality (NRC 2004) and is suitable for climate research and application (Knapp 2008; Knapp et al. 2011; Raghavendra et al. 2018), particularly over northern and central Africa (Knapp et al. 2011; Raghavendra et al. 2018). Note that the GridSat-B1 Tb is available from 1982–present, but the period 1982–1985 is excluded from this analysis due to the relatively higher frequency of missing data when compared to other years, and the abnormal low T_b values associated with the 1982 eruption of El Chichón volcano. Similarities in the assessment of MJO characteristic from the CPC and GridSat-B1 datasets should improve the confidence in the results presented in this study.

3 Methods

The methods used to analyze the abovementioned datasets are purely statistical. The temporal trends in precipitation and cloud cover were established using multiple linear regression and their statistical significance (p-value) were assessed using a two-tailed Student's t test. As the linear trend is sensitive to the start/end points of the data series, when applicable, the non-parametric (distribution-free) Mann–Kendall (MK) test (Hirsch et al. 1982), which overcomes the abovementioned limitation, was also applied to check the significance of the trend. The analysis presented in this study is limited to the months ranging from October–March since the MJO signal and RMM amplitude are significantly stronger during this period (e.g., Adames et al. 2016; Zhang and Dong 2004). These months contain the rainiest month of October, the December–February (DJF) dry season, and the start of the wet season around March as the tropical rainbelt over the Congo migrates southward during October to January, and northward back towards the basin during February to April (e.g., Washington et al. 2013; Nicholson 2018).

In this paper, the interannual variability of the seasonal rainfall and number of days in each MJO category is broken down using the MJO RMM phase and RMM amplitude. The total number of days in each season may be decomposed as the sum of the number of wet (RMM phase 2), dry (RMM phases 5 and 6), inactive (RMM amplitude < 1), and other (RMM phases 1, 3, 4, 7 and 8) MJO days i.e., $All\ days = MJO_{wet\ days} + MJO_{dry\ days} + MJO_{inactive\ days} + MJO_{other\ days}$. A similar approach was applied to decompose the total seasonal rainfall for each year i.e., $PR_{total} = PR_{wet\ days} + PR_{dry\ days} + PR_{inactive\ days} + PR_{other\ days}$ (Note: precipitation is abbreviated as "PR"). The rainfall during these four types of MJO days contributes to the overall seasonal rainfall which is outlined below. First, Oct–Mar daily average seasonal rainfall ($\overline{PR}$) for each year is decomposed as the fractional sum of the daily average rainfalls observed during the wet, dry, inactive, and remainder (other) MJO days i.e.,

$$\begin{aligned}\overline{PR}_{total} = &\Big(\Big(MJO_{wet\ days} \times \overline{PR}_{wet\ days}\Big) + \Big(MJO_{dry\ days} \times \overline{PR}_{dry\ days}\Big) \\ &+ \Big(MJO_{inactive\ days} \times \overline{PR}_{inactive\ days}\Big) + \Big(MJO_{other\ days} \times \overline{PR}_{other\ days}\Big)\Big) \\ &\div All\ days.\end{aligned} \tag{1}$$

Applying Eq. 1 for all 40 years of data yields a time-series that breakdowns the daily average seasonal rainfall as the sum of four parts defined by the RMM phase and amplitude.

Next, we may categorically extract the association of the MJO signature to the overall rainfall trend by excluding one term at a time in the right-hand side (R.H.S.) of Eq. 1. For instance, the contribution of $MJO_{dry\ days}$ may be assessed by omitting the second term in the R.H.S. of Eq. 1 and subtracting $MJO_{dry\ days}$ from $All\ days$ in Eq. 1 i.e., $\overline{PR}_{total-dry} = \Big(\Big(MJO_{wet\ days} \times \overline{PR}_{wet}\Big) + \Big(MJO_{inactive\ days} \times \overline{PR}_{inactive}\Big) + \Big(MJO_{other\ days} \times \overline{PR}_{other}\Big)\Big) \div \Big(All\ days - MJO_{dry\ days}\Big)$. An estimate of a lower bound of the MJO categories' contribution is quantified by calculating the percentage difference in the slopes of the linear trend for a given category and compared to the $All\ days$ trend. A similar approach was

also applied for fractional cloud cover derived from the GridSat-B1 dataset.

4 Results

4.1 Interactions between the MJO and the seasonal cycle of rainfall

Since the Congo is situated along the Equator, the region is characterized by a bimodal precipitation distribution (i.e., two dry and two wet seasons per year) modulated by the migration of the tropical rainbelt (Fig. 1a; Washington et al. 2013; Nicholson 2018; Jiang et al. 2019). The wet seasons include the months of March, April, and May (MAM) and September, October, and November (SON), while the dry season is composed of December, January, and February (DJF), and June, July, and August (JJA). Figure 1a shows the seasonal cycle over the Congo characterized by high interannual variability with deviations frequently exceeding ~ 25% when compared to the climatological mean. The long-term drying signal is also evident in the rainfall record i.e., the monthly mean rainfall from the period 2009–2018 is considerably below the 1979–1988 mean (e.g., Zhou et al. 2014; Hua et al. 2016; Nicholson et al. 2018; Jiang et al. 2019).

The relationships between the MJO categories as defined in this paper and daily mean seasonal average rainfall over the Congo are presented in the form of a boxplot in Fig. 1b. A combination of the sample sizes and inter-quartile ranges of the distribution are used to assess statistical significance (McGill et al. 1978). Figure 1b shows significantly higher rainfall amounts during the wet phase, and the lowest median rainfall amounts for MJO dry days when compared to all other MJO categories. Rainfall during inactive and other MJO days are very similar and appears to have a neutral impact on rainfall over the Congo. The combined influences between the seasonal cycle and MJO RMM phases is shown in Fig. 1c. In other words, Fig. 1c illustrates the precipitation impact associated with the phasing of the MJO coinciding with the seasonal migration of the tropical rainbelt over Central Africa.

To better assess the impact of the RMM phases on rainfall, precipitation anomalies were generated by first calculating the seasonal cycle using five harmonic components to the annual cycle and then subtracting the seasonal cycle from the raw precipitation (methods outlined in Roundy 2017 and Raghavendra et al. 2019). While the daily mean rainfall is generally higher during the months of MAM and SON, and lower during the months of DJF and JJA (Fig. 1a), there are strong rainfall anomalies across different MJO RMM phases during different seasons (Fig. 1d). While the migration of the tropical rainbelt strongly dictates seasonal rainfall amounts and thunderstorm activity (e.g., Nicholson 2018; Taylor et al. 2018) across all RMM phases, there is a significant distinction between rainfall amounts observed during the wet and dry RMM phases across different months of the year. Rainfall is typically enhanced during the wet RMM phases and reduced during the dry RMM phases.

Since the tropical rainbelt (Nicholson 2018) and the MJO serve as important dynamic–thermodynamic forcing mechanisms regulating tropical rainfall (e.g., Madden and Julian 1972; Zhang and Dong 2004; Barnes et al. 2015; Adames et al. 2016), it is not surprising to observe the synchronized seasonality and differences in rainfall across different RMM phases over the Congo (Fig. 1c, d; e.g., Pohl and Camberlin 2006a, b; Berhane and Zaitchik 2014; Pohl et al. 2018). However, some of the strongest modulations of rainfall may be attributable to the MJO RMM phases from Oct–Mar. This relationship is weak during other months and likely results from other forcing mechanisms such as the onset of the West African monsoon, which dominates the circulation between May–Aug (Sultan and Janicot 2003). For the Oct–Mar period, rainfall during MJO RMM phase 2 as the wet phase with positive rainfall anomalies, and RMM phase 5 and 6 as the dry phases with negative rainfall anomalies show statistically significant differences (Fig. 1b). While the results are sensitive to choices in three parameters i.e., season, cut-off RMM amplitude applied to define an active or inactive MJO days, and practical choices for RMM phases used to define the wet and dry MJO spell, these choices do not impact the overall conclusions presented in this paper.

4.2 Spatial composite analysis of wet and dry MJO days

The wet and dry MJO days over the Congo are associated with significantly different circulation patterns (Fig. 2). During wet MJO days, westerly wind anomalies dominate the lower troposphere (850 hPa) and were associated with the injection of moisture from the Atlantic Ocean into the Congo basin. Recent studies such as Dyer et al. (2017) have also found a strong association between westerly wind anomalies from the Atlantic Ocean and positive rainfall anomalies over the Congo. There is also a strong convergence-divergence dipole located near Lake Victoria and East-African Highlands during wet MJO days (Fig. 2a). Since thunderstorms usually form over the East-African Highlands during the late-afternoon (e.g., Hill and Lin 2003) and are steered westward by the prevailing lower tropospheric easterly flow (e.g., Corfidi et al. 1996), the invigorated circulation may likely promote thunderstorm development by increasing the windshear (e.g., Taylor et al. 2018). At the same time, westerly wind anomalies may act to reduce the strength of the background easterly flow which slows down the propagation speed of thunderstorm cells over the Congo. These intense and relatively slow propagating thunderstorms cell likely

increase the rainfall amount over the Congo. The lower tropospheric circulation anomaly reverses during dry MJO days. This reversal in circulation likely advects drier continental airmass from northern and eastern Africa which in turn suppresses thunderstorm activity over the Congo during dry phases. Figure 2 also compliments the findings of Fig. 1b–d by showing wet RMM phases are associated with positive rainfall anomalies and vice versa.

From the standpoint of seasonal to sub-seasonal variability, since the number of days during Oct–Mar (i.e., ~ 182 days) may allow for multiple MJO episodes with time windows ranging from 30 to 60 days (Madden and Julian 1971, 1972; Wheeler and Kiladis 1999), there exists potentially 3–6 time windows during which the MJO may substantially enhance or suppress precipitation amounts over Africa. An important argument to be considered is whether random variability in MJO activity intersecting with the migration of the tropical rainbelt would produce a long-term low frequency trend in rainfall. The crux of this paper includes how trends in MJO activity may contribute to the overall observed precipitation trend over the Congo during the months of Oct–Mar. These arguments are explored in more detail in Sects. 4.3 and 4.4.

4.3 A brief overview of the MJO categories and corresponding rainfall

An overview of the interannual variability of the MJO days and rainfall by category are presented in Fig. 3. During the period of study, the overall occurrence of MJO wet days was 7.82%, dry days was 17.6%, inactive days (i.e., RMM amplitude < 1) was 35.7%, and other days was 39.2%. Dry days are more frequent when compared to wet days since two RMM phases (i.e., phases 5 and 6) were regarded as dry phases, but only one RMM phase (i.e., phase 2) was regarded as dry phase. The definitions for the different MJO categories used in this study result in a large number of inactive and other days and are consistent with the findings of similar studies using the RMM index (e.g., LaFleur et al. 2015). In Fig. 3a, number of days in a season vary between 182 (regular year) and 183 (leap year), therefore the total number days (*All days*) is constant in time. This however is not the case for rainfall, which shows considerable year-to-year variability and a strong drying trend (Fig. 3b). The percentage-based breakdown of MJO days is presented in Fig. 3c. Since there is practically no variability in the

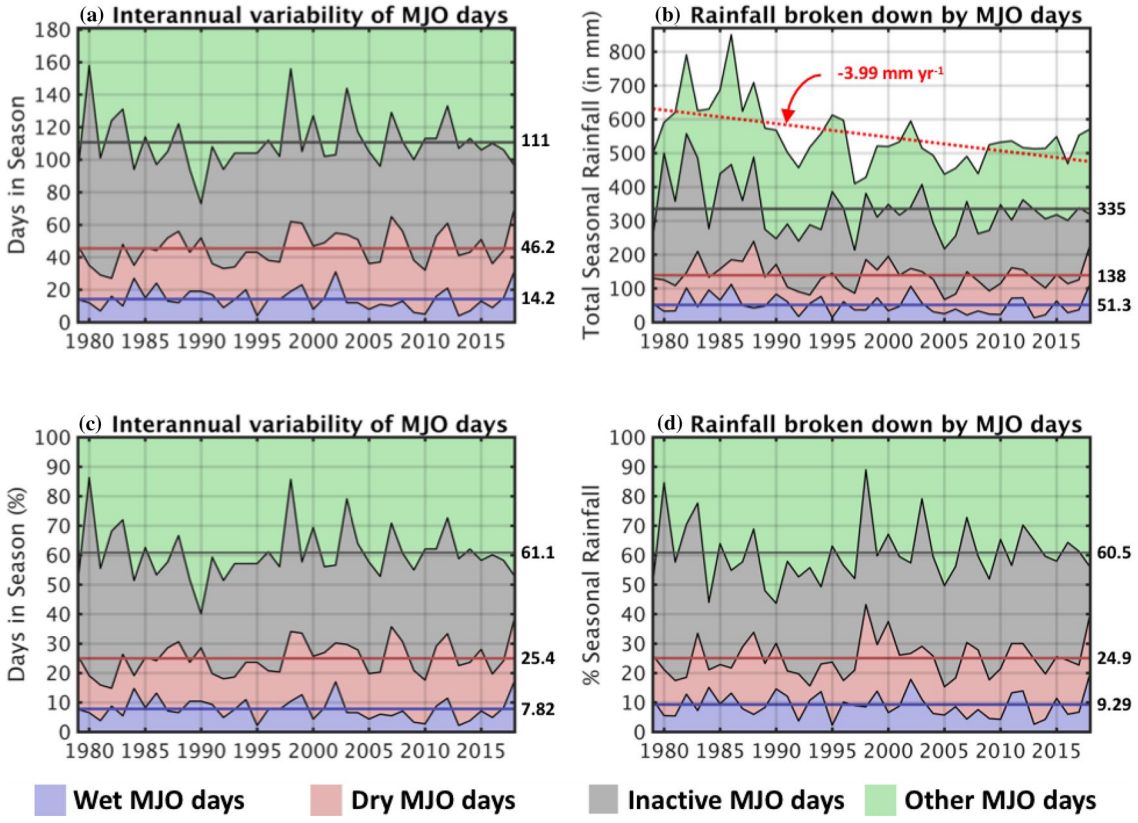

Fig. 3 Stacked area plot showing the Oct–Mar raw and percentage based interannual variability decomposed by MJO category for **a**, **c** MJO days, and **b**, **d** rainfall. The solid line represents the categorically integrated climatological mean. The trend in total seasonal rainfall amount is depicted using a dotted red line in **b**

total number of days per season, Fig. 3a, c are identical. Similar to Fig. 3b, a percentage-based breakdown for rainfall by MJO category is presented in Fig. 3d. The substantial year-to-year variability and trend in rainfall however results in some differences between Fig. 3b, d. The percentage-based breakdown of rainfall by MJO category is as follows: 9.29% for wet days, 15.7% for dry days, 35.6% for inactive days, and 39.2% for other days. In other words, rainfall amount by MJO category closely follows the number of MJO days in each category. However, on average 7.82% of MJO wet days bring 9.29% of the total rainfall while 17.6% of MJO dry days bring 15.7% of the total rainfall. The fraction of rainfall from inactive and other days align almost perfectly with the fractional breakdown of the number of inactive and other days (Figs. 1b, 3c, d).

As shown in Figs. 1 and 2, rainfall is significantly enhanced during wet MJO days, and suppressed during dry MJO days. This relationship is also extractable from Fig. 3 by comparing the fractional contribution of rainfall from the corresponding MJO category. Therefore, a reasonable hypothesis to consider includes: do seasons characterized by larger number of wet or dry MJO days result in significantly different seasonal rainfall anomalies? To answer this question, the correlation between the number of wet and dry MJO days, and the seasonal rainfall anomaly are presented in Fig. 4. Results suggest an increase in the number of wet MJO days is characterized by a positive rainfall anomaly ($R = +0.26$ and p value $= 0.10$), while an increase in the number of dry MJO days is characterized by a negative rainfall anomaly ($R = -0.30$ and p value $= 0.06$). In sum, the effect of wet MJO and dry MJO days may be evaluated by calculating the difference in the number of wet and dry MJO days for each year normalized by the number of RMM phases used. The difference in the number of wet and dry MJO days and rainfall anomaly shows a stronger relationship ($R = +0.35$ and p value $= 0.03$) when compared to the individual parts. Overall, Fig. 4 demonstrates a significant correlation between the number of wet and dry MJO days and observed rainfall over the Congo.

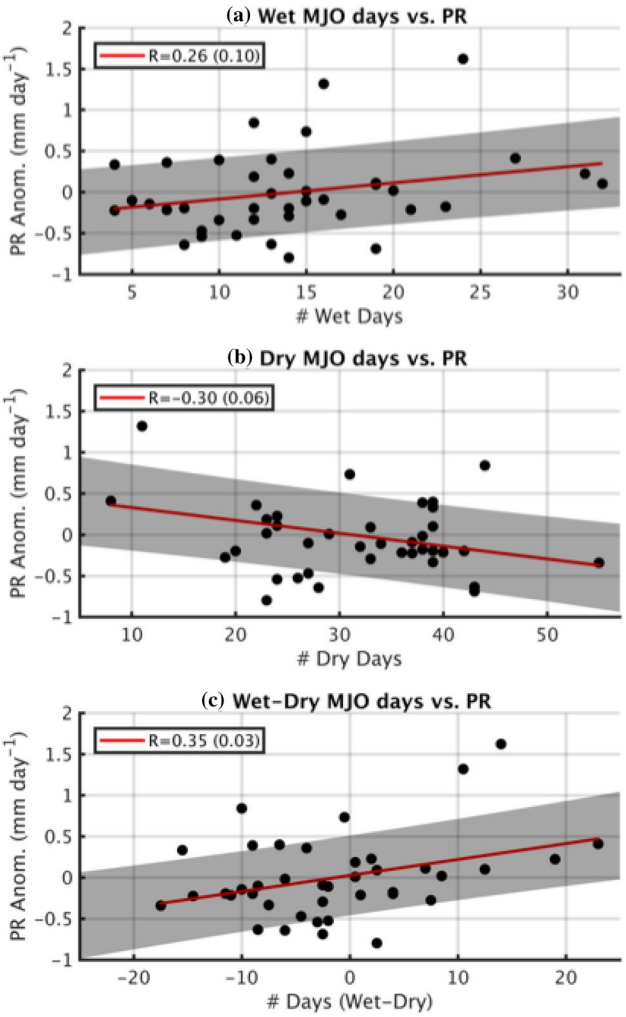

Fig. 4 Scatter plot showing the relationship between the Oct–Mar mean rainfall anomaly and **a** number of wet MJO days, **b** number of dry MJO days, and **c** difference between the number of wet and dry MJO days normalized by the number of RMM phases chosen for wet and dry RMM phases from 1979–2018. The linear regression line (red line), correlation coefficient (R) with significance level (p value in parentheses), and ± 25% of the regression prediction interval (gray shading; technical documentation available at https://www.mathworks.com/help/curvefit/cfit.predint.html) are displayed in each panel

4.4 Categorical evaluation of trends in MJO days and rainfall

Attributing rainfall to a single mechanism (e.g., the MJO) is likely an impossible task given the complex, coupled and sometimes competing interactions observed among different controlling factors in the tropical atmosphere (e.g., Roundy 2012; Holton and Hakim 2013). However, by calculating the daily average seasonal rainfall by omitting iteratively one of four types of MJO days (i.e., wet, dry, inactive, and other days) and comparing it to the overall mean rainfall trend (see Eq. 1 and Sect. 3), a useful starting point is developed in this paper to quantify the impact of the trends in MJO activity on rainfall over the Congo. The rainfall variability captured by the individual parts in Eq. 1 was able to reproduce 100% of the total observed rainfall.

The interannual variability across seasons in the number of active MJO wet (W) and dry (D) days, W–D days, rainfall anomaly, and rainfall anomaly during an active MJO are presented in Fig. 5a. From 1979–2018, Oct–Mar shows a significant increase in the number of dry MJO days. Similar to the results presented in Fig. 4, the trend of the difference in the number of wet and dry MJO days is stronger when

compared to the trends in the number of dry MJO days. The trends in the number of MJO days for each category is explicitly presented in Fig. 5b. Only dry MJO days show a significant increase of 0.34 days year^{-1} from 1979–2018. While rainfall over the Congo has decreased during all seasons (e.g., Hua et al. 2016; Jiang et al. 2019), these results suggests that the declining rainfall trend is likely enhanced by the MJO. Notwithstanding a strong role by large-scale mechanisms outside MJO dynamics (e.g., SSTs, IOD, and the Walker circulation; Hua et al. 2016, 2018; Creese et al. 2019) in modulating rainfall over the Congo, the increasing trend in the number of dry MJO days is acting to strengthen the overall drying trend over the Congo (Figs. 1b, 2, and 4).

In Fig. 6, the mean Oct–Mar rainfall shows a significant decreasing trend consistent with the enhanced subsidence observed over the Congo (Hua et al. 2016; Raghavendra et al. 2018). This trend persists even if the variability attributable to the MJO is categorically removed. When compared to the overall mean rainfall trend (−0.21 mm day^{-1} decade^{-1}), the slope of the rainfall trend is practically unchanged with the removal of wet MJO days, 13% weaker with the removal of dry MJO days (−0.18 mm day^{-1} decade^{-1}), 21% stronger with the removal of inactive MJO days (−0.26 mm day^{-1} decade^{-1}), and 3.8% weaker with the removal of other MJO days (−0.21 mm day^{-1} decade^{-1}). The strong contribution from dry and inactive MJO days was expected considering the significantly increasing trend

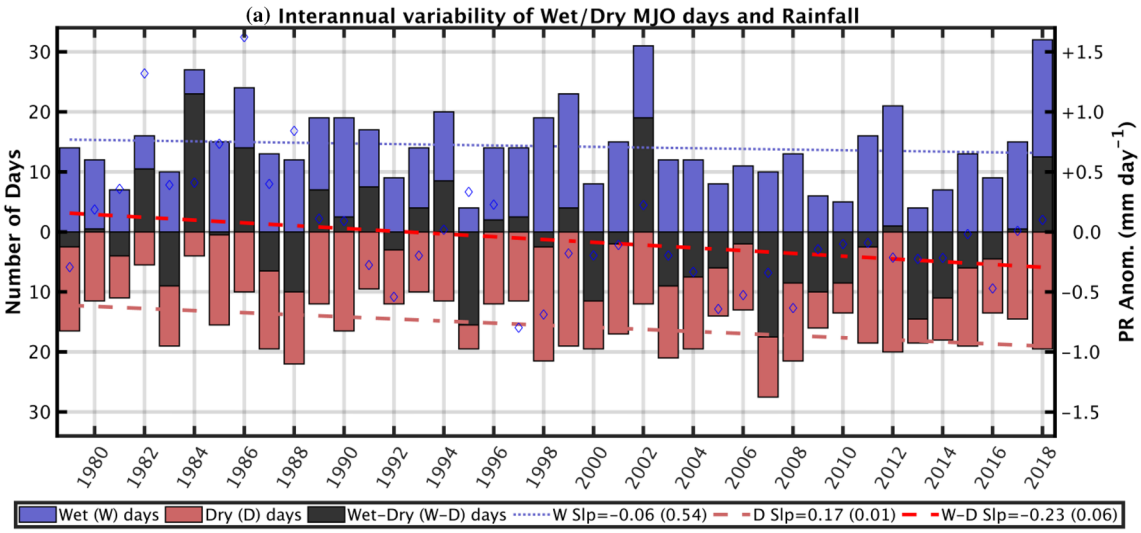

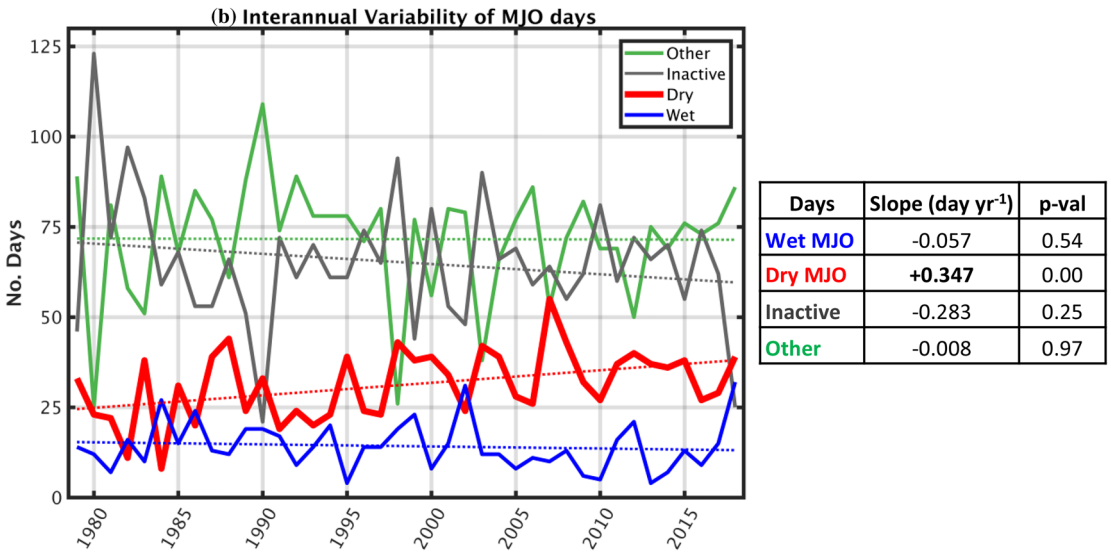

Days	Slope (day yr^{-1})	p-val
Wet MJO	-0.057	0.54
Dry MJO	**+0.347**	0.00
Inactive	-0.283	0.25
Other	-0.008	0.97

Fig. 5 **a** Interannual variability in the number of MJO wet (blue), dry (red), and wet–dry days (grey bar) normalized by the number of RMM phases used. Precipitation anomaly (PR; mm day^{-1}; blue circles) from 1979–2018 is displayed against the right vertical axis. The slope of the trend line and p value (in parentheses) are displayed in the legend. **b** Interannual variability and trend of MJO days by category. The slope (bold indicates significant trend as per the MK-test) and p value for trend lines are displayed next to **b**

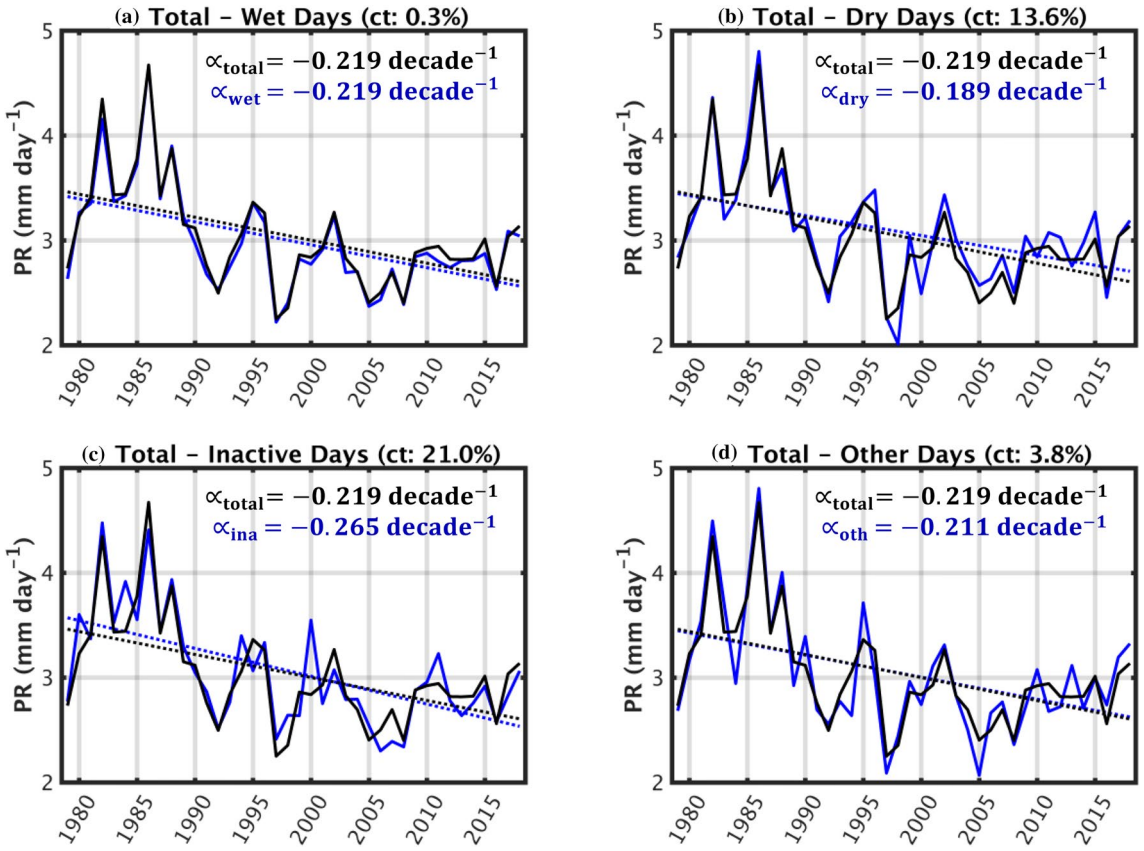

Fig. 6 Interannual variability and linear trend in the Oct–Mar mean rainfall (black line) with **a** wet days, **b** dry days, **c** inactive days, and **d** other MJO days categorically removed from the overall timeseries (blue line). The slope for trend lines are displayed within each panel. The title in **a**–**d** also shows the % contribution (ct) to the overall rainfall trend for each MJO category removed from the reconstruction

in dry MJO days (+ 3.47 days decade^{-1}) and decreasing (albeit statistically insignificant) trend in inactive MJO days (− 2.83 days decade^{-1}; Fig. 5b).

There are very few reliable and long-term rainfall datasets over the Congo at daily or higher resolution. Furthermore, there is considerable spread amongst model (reanalysis) derived rainfall estimates over the Congo (e.g., Washington et al. 2013; Lee and Biasutti 2014; Alsdorf et al. 2016; Nicholson et al. 2018; Hua et al. 2019). Therefore, cloud cover is used as a proxy for thunderstorm and rainfall from a high-quality satellite dataset. Results obtained by applying Eq. 1 to the areal extent of cold cloud tops derived from the GridSat-B1 dataset concur with the findings using rainfall data (Fig. 7). As in Fig. 6, when compared to the overall cloud cover trend (− 0.47% decade^{-1}) from 1986–2018, the slope of the rainfall trend is practically unchanged with the removal of wet MJO days, 14% weaker with the removal of dry MJO days (− 0.40% decade^{-1}), 8.4% stronger with the removal of inactive MJO days (− 0.51% decade^{-1}), and 3.8% weaker with the removal of other MJO days (− 0.53% decade^{-1}; Fig. 7).

5 Concluding remarks

Since the MJO is an important dynamic-thermodynamic forcing operating on the seasonal/sub-seasonal timescale (e.g., Barnes et al. 2015; Madden and Julian 1972), this paper aimed to study precipitation variability and trends from a seasonal/sub-seasonal prospective over the Congo by analyzing the role of the MJO. First, the overall climatological impact of the MJO on rainfall over the Congo using four MJO categories (i.e., wet, dry, inactive, and other) from Oct–Mar from 1979–2018 are explored in Figs. 1, 2, 3. The phasing of the tropical rainbelt over Africa with the different RMM phases of the MJO was also analyzed in Fig. 1c, d. The relationship between rainfall and the number of wet and dry MJO days (Fig. 4), and the interannual variability and trends in the MJO days (Figs. 5, 6, 7) suggests a non-trivial impact from the increase in the number of dry MJO days on the seasonal rainfall observed over the Congo. While changes in the large-scale circulation of the atmosphere and other teleconnections are important in determining rainfall trends over the Congo across decadal and multi-decadal

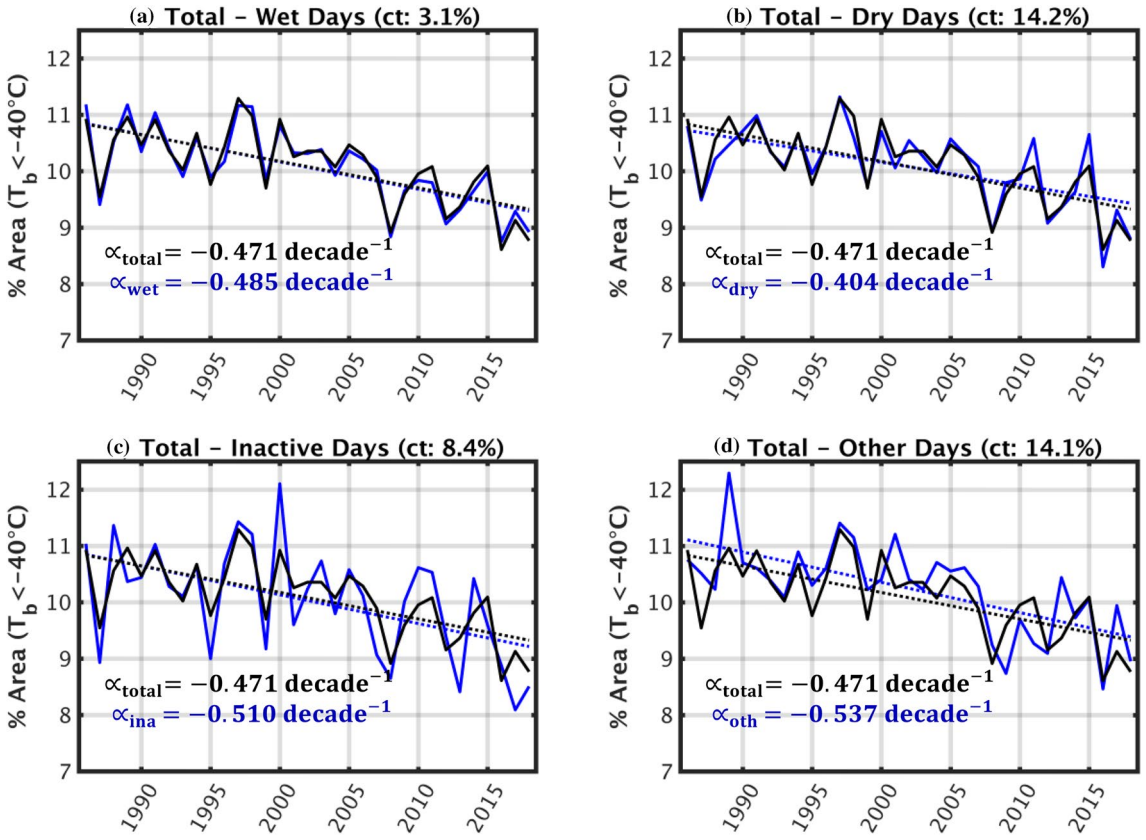

Fig. 7 Interannual variability and linear trend in the Oct–Mar areal extent of cold cloud cover (black line) with **a** wet days, **b** dry days, **c** inactive days, and **d** other MJO days categorically removed from the overall timeseries (blue line). The slope for trend lines are displayed within each panel. The title in **a**–**d** also shows the % contribution (ct) to the total cold cloud cover trend for each MJO category removed from the reconstruction

timescales (e.g., Hua et al. 2016, 2018; Creese et al. 2019), this study demonstrates that trends and changes in seasonal/sub-seasonal variability (e.g., the MJO and other CCAEW; Raghavendra et al. 2019) in both the present and future climate are also equally important for the rainfall totals and overall wellbeing of the Congo rainforest.

The impact of the MJO on rainfall is quantified by evaluating the contribution from each of the four MJO categories to the overall seasonal rainfall trend. Though the Wheeler and Hendon (2004) MJO RMM index is not a direct measure of Congo rainfall, the algorithm used here uses Congo rainfall data to distinguish between the favored local moist or dry phases of the RMM index. While multiple rainfall and vegetation datasets shows a significant trend towards drier conditions (e.g., Zhou et al. 2014; Jiang et al. 2019), RMM index data suggest an increasing trend in the number of days in dry phases for equatorial Africa over time. Trends in the RMM data compliment the large-scale drying over the Congo (e.g., Hua et al. 2016) even though the RMM index data implies little explicitly about Congo rainfall. In other words, changes in the MJO over time may explain some of the change in rainfall since the declining trend in rainfall is smaller if the dry MJO days were removed (Figs. 5, 6, 7).

Results suggest that the trends in the number of dry MJO days may contribute 13.6% to amplify the overall Oct–Mar declining rainfall trend over the Congo (Figs. 5, 6). Since there are few products and large uncertainties for rainfall estimates over the Congo, cloud cover from the GridSat-B1 T_b dataset was used as a proxy for rainfall. The analysis of cloud cover suggests that the trends in the number of dry MJO days may contribute approximately 14.2% to the Oct–Mar fractional cloud cover trend over the Congo. While attributing precipitation to the MJO or other tropical waves is difficult since it is not possible to completely associate tropical rainfall with singular physical mechanisms, the long-term trends in the relationship between rainfall over the Congo and the impact of the MJO appear robust. Given the significant relationship between the MJO and rainfall over the Congo (Figs. 1, 2, 3), one may conclude that the rainfall trends observed over the Congo are at least partially enhanced by a significant increase in the number of dry MJO days.

Consistent with previous findings (e.g., Pohl and Camberlin 2006b), the MJO may significantly enhance or suppress rainfall over the Congo. Therefore, studying such interactions from a present and future climate prospective is crucial to improving our understanding and future climate projections of rainfall and ecology over the Congo rainforest. It is however difficult using existing climate models (e.g., the models used in CMIP5) which are unable to properly simulate large-scale disturbances such as the MJO (Hung et al. 2013). This will remain as a big challenge to predict the future climate over the Congo until climate models are significantly improved to simulate tropical rainfall and its interaction with the rainbelt, and able to simulate modes of tropical variability such as the MJO and other CCAEW.

Acknowledgements Authors AR, LZ, and YJ were supported by National Science Foundation (NSF AGS-1535426 and AGS-1854486). PR would like to acknowledge the support received from NSF AGS-1128779 and AGS-1358214. We thank Dr. Susanna Corti for serving as the Editor of this paper, and two anonymous reviewers for their constructive feedback which greatly improved the quality of this paper.

References

Adames AF, Wallace JM, Monteiro JM (2016) Seasonality of the structure and propagation characteristics of the MJO. J Atmos Sci 73:3511–3526

Alsdorf D et al (2016) Opportunities for hydrologic research in the Congo Basin. Rev Geophys 54:378–409

Barnes HC, Zuluaga MD, Houze RA (2015) Latent heating characteristics of the MJO computed from TRMM observations. J Geophys Res 120:1322–1334

Berhane F, Zaitchik B (2014) Modulation of daily precipitation over East Africa by the Madden–Julian Oscillation. J Climate 27:6016–6034

Chen D, Dai A (2019) Precipitation characteristics in the Community Atmosphere Model and their dependence on model physics and resolution. J Adv Model Earth Syst 11:2352–2374

Corfidi SF, Merritt JH, Fritsch JM (1996) Predicting the movement of mesoscale convective complexes. Weather Forecast 11:41–46

Creese A, Washington R, Jones R (2019) Climate change in the Congo Basin: processes related to wetting in the December–February dry season. Climate Dyn 53:3583–3602

Dai A (2006) Precipitation characteristics in eighteen coupled climate models. J Climate 19:4605–4630

Dee DP, Uppala SM, Simmons AJ et al (2011) The ERA-Interim reanalysis: configuration and performance of the data assimilation system. Q J R Meteorol Soc 137:553–597

Dyer ELE, Jones DBA, Nusbaumer J, Li H, Collins O, Vettoretti G, Noone D (2017) Congo Basin precipitation: assessing seasonality, regional interactions, and sources of moisture. J Geophys Res Atmos 122:6882–6898

Gottschalck J, Wheeler M, Weickmann K, Vitart F, Savage N et al (2010) A framework for assessing operational Madden–Julian oscillation forecasts: a CLIVAR MJO working group project. Bull Am Meteorol Soc 91:1247–1258

Hamada A, Takayabu YN, Liu C, Zipser EJ (2015) Weak linkage between the heaviest rainfall and tallest storms. Nat Commun 6:6213

Held IM, Soden BJ (2006) Robust responses of the hydrological cycle to global warming. J Climate 19:5686–5699

Hill CM, Lin Y-L (2003) Initiation of a mesoscale convective complex over the Ethiopian Highlands preceding the genesis of Hurricane Alberto (2000). Geophys Res Lett 30:1232

Hirsch RM, Slack JR, Smith RA (1982) Techniques of trend analysis for monthly water quality data. Water Resour Res 18:107–121

Holton JR, Hakim GJ (2013) An introduction to dynamic meteorology. Elsevier, Amsterdam

Hua W, Zhou L, Chen H, Nicholson SE, Raghavendra A, Jiang Y (2016) Possible causes of the Central Equatorial African long-term drought. Environ Res Lett 11:124002

Hua W, Zhou L, Chen H, Nicholson SE, Jiang Y, Raghavendra A (2018) Understanding the Central Equatorial African long-term drought using AMIP-type simulations. Climate Dyn 50:1115–1128

Hua W, Zhou L, Nicholson SE, Chen H, Qin M (2019) Assessing reanalysis data for understanding rainfall climatology and variability over Central Equatorial Africa. Climate Dyn 53:651–669

Hung M, Lin J, Wang W, Kim D, Shinoda T, Weaver S (2013) MJO and convectively coupled equatorial waves simulated by CMIP5 climate models. J Climate 26:6185–6214

Jackson B, Nicholson SE, Klotter D (2009) Mesoscale convective systems over western equatorial Africa and their relationship to large-scale circulation. Mon Weather Rev 137:1272–1294

Jiang Y, Zhou L, Tucker CJ, Raghavendra A, Hua W, Liu Y, Joiner J (2019) Widespread increase of boreal summer dry season length over the Congo rainforest. Nat Climate Change 9:617–622

Knapp KR (2008) Scientific data stewardship of International Satellite Cloud Climatology Project B1 global geostationary observations. J Appl Remote Sens 2:023548

Knapp KR et al (2011) Globally gridded satellite observations for climate studies. Bull Am Meteorol Soc 92:893–907

LaFleur DM, Barrett BS, Henderson GR (2015) Some climatological aspects of the Madden–Julian Oscillation (MJO). J Climate 28:6039–6053

Lee DE, Biasutti M (2014) Climatology and variability of precipitation in the twentieth-century reanalysis. J Climate 27:5964–5981

Lewis SL (2006) Tropical forests and the changing earth system. Philos Trans R Soc Lond B 361:195–210

Lewis SL et al (2009) Increasing carbon storage in intact African tropical forests. Nature 457:1003–1006

Madden R, Julian P (1971) Detection of a 40–50 day oscillation in the zonal wind in the tropical Pacific. J Atmos Sci 28:702–708

Madden R, Julian P (1972) Description of global-scale circulation cells in the tropics with a 40–50 day period. J Atmos Sci 29:1109–1123

McGill R, Tukey JW, Larsen WA (1978) Variations of boxplots. Am Stat 32:12–16

Nicholson SE (2018) The ITCZ and the seasonal cycle over equatorial Africa. Bull Am Meteorol Soc 30:337–348

Nicholson SE, Klotter D, Dezfuli AK, Zhou L (2018) New rainfall datasets for the Congo Basin and surrounding regions. J Hydrometeorol 19:1379–1396

Pohl B, Camberlin P (2006a) Influence of the Madden–Julian Oscillation on East African rainfall. I: intraseasonal variability and regional dependency. Q J R Meteorol Soc 132:2521–2539

Pohl B, Camberlin P (2006b) Influence of the Madden–Julian oscillation on East Africa rainfall. II: March–May season extremes and interannual variability. Q J Roy Meteorol Soc 132:2541–2558

Pohl B, Dieppois B, Crétat J, Lawler D, Rouault M (2018) From synoptic to interdecadal variability in Southern African rainfall: toward a unified view across time scales. J Climate 31:5845–5872

Raghavendra A, Zhou L, Schiraldi NJ, Roundy PE (2017) MJO phase speed and rainfall variability over the Congo rainforest. In: Fifth symposium on prediction of the madden-julian oscillation: processes, prediction and impact Poster#355 American

Meteorological Society. https://ams.confex.com/ams/97Annual/webprogram/Paper302854.html
Raghavendra A, Zhou L, Jiang Y, Hua W (2018) Increasing extent and intensity of thunderstorms observed over the Congo Basin from 1982 to 2016. Atmos Res 213:17–26
Raghavendra A, Roundy PE, Zhou L (2019) Trends in tropical wave activity from 1980s–2016. J Climate 32:1661–1676
Roundy PE (2012) Observed structure of convectively coupled waves as a function of equivalent depth: Kelvin waves and the Madden–Julian oscillation. J Atmos Sci 69:2097–2106
Roundy PE (2017) Diagnosis of seasonally varying regression slope coefficients and application to the MJO. Q J Roy Meteorol Soc 143:1946–1952
Schlueter A, Fink AH, Knippertz P, Vogel P (2019a) A systematic comparison of tropical waves over Northern Africa. Part I: influence on rainfall. J Climate 32:1501–1523
Schlueter A, Fink AH, Knippertz P (2019b) A systematic comparison of tropical waves over northern Africa. Part II: dynamics and thermodynamics. J Climate 32:2605–2625
Sinclaire Z, Lenouob A, Tchawouaa C, Janicotc S (2015) Synoptic Kelvin type perturbation waves over Congo basin over the period 1979–2010. J Atmos Sol Terr Phys 130–131:43–46
Sultan B, Janicot S (2003) West African monsoon dynamics. Part II: the "pre-onset" and the "onset" of the summer monsoon. J Climate 16:3407–3427
Taylor KE, Stouffer RJ, Meehl GA (2012) An overview of CMIP5 and the experiment design. Bull Am Meteorol Soc 93:495–498
Taylor CM et al (2017) Frequency of extreme Sahelian storms tripled since 1982 in satellite observations. Nature 544:475–478
Taylor CM et al (2018) Earlier seasonal onset of intense Mesoscale Convective Systems in the Congo Basin since 1999. Geophys Res Lett 45:13458–13467
Ventrice MJ, Thorncroft CD, Janiga MA (2012) Atlantic tropical cyclogenesis: a three-way interaction between an African easterly wave, diurnally varying convection, and a convectively coupled atmospheric Kelvin wave. Mon Weather Rev 140:1108–1124
Washington R, James R, Pearce H, Pokam WM, Moufouma-Okia W (2013) Congo Basin rainfall climatology: can we believe the climate models? Philos Trans R Soc B 368:20120296
Wheeler MC, Hendon HH (2004) An all-season real-time multivariate MJO index: development of an index for monitoring and prediction. Mon Weather Rev 132:1917–1932
Wheeler M, Kiladis GN (1999) Convectively coupled equatorial waves: analysis of clouds and temperature in the wavenumber–frequency domain. J Atmos Sci 56:374–399
Zaitchik BF (2016) Madden–Julian Oscillation impacts on tropical African precipitation. Atmos Res 184:88–102
Zhang C, Dong M (2004) Seasonality of the Madden–Julian oscillation. J Climate 17:3169–3180
Zhou L et al (2014) Widespread decline of Congo rainforest greenness in the past decade. Nature 509:86–90
Zipser E, Liu C, Cecil D, Nesbitt S, Yorty D (2006) Where are the most intense thunderstorms on Earth? Bull Am Meteorol Soc 87:1057–1071